EVALUATION OF INFRARED CANOPY TEMPERATURE DATA IN RELATION TO SOIL WATER-BASED IRRIGATION SCHEDULING IN A HUMID SUBTROPICAL CLIMATE

B. P. Lena, B. V. Ortiz, A. F. Jiménez-López, Á. Sanz-Sáez,
S. A. O'Shaughnessy, M. K. Durstock, G. Pate

Beyond 2020, VISION OF THE FUTURE
Collection
Research

HIGHLIGHTS

- Corn response to irrigation was influenced by the precipitation distribution in 2018 and 2019, and that impacted the response of CWSI as an irrigation scheduling signaling method.
- CWSI was sensitive to changes in soil water storage, increasing due to crop evapotranspiration and decreasing after a precipitation or irrigation event.
- In 2018, both seasonal CWSI and yield were not different among the irrigation treatments, while in 2019, seasonal CWSI and yield were all statistically different among the treatments evaluated.
- Post analysis of canopy and air temperature indicated that the temperature-time threshold (TTT) method might not appropriately signal crop water stress in a humid environment.

ABSTRACT. *Irrigation scheduling based on the crop water stress index (CWSI) and temperature-time threshold (TTT) methods is promising for semi-arid and arid climates. The objective of this study was to investigate if CWSI and TTT methods could be used as irrigation signaling tools for a humid environment in the southeastern U.S. Corn canopy temperature data were collected in Alabama in 2018 and 2019 using infrared leaf temperature sensors on a fully irrigated treatment and on two limited irrigation treatments. A set of three soil water sensors installed at 0.15, 0.3, and 0.6 m soil depth were used to prescribe irrigation time and amount. CWSI was sensitive to precipitation, irrigation, and plant water uptake. No statistical differences in CWSI or yield among the three irrigation levels were found in 2018 when precipitation was well distributed during the season. In contrast, during 2019 both CWSI and yield differed significantly among the three irrigation treatments. Precipitation events in 2019 were sparse compared to 2018; therefore, irrigation promoted greater differences in water availability between treatments. Inconsistencies observed in potential irrigation signaling using the TTT method with or without the inclusion of a limiting relative humidity algorithm indicate that the TTT method may not be a reliable irrigation signaling tool for humid environments.*

Keywords. *Corn yield, Crop water stress index, Irrigation scheduling, Limiting relative humidity, Soil water depletion, Temperature-time threshold.*

Irrigation plays an important role in crop production in the U.S. Even though only 17% of the total harvested cropland (21.8 million ha) is irrigated, irrigated crop production contributed 38.6% of the total market value of agricultural products sold in the country in 2017 (USDA, 2017). In Alabama, total irrigated land increased from 46,000 to 58,000 ha from 2012 to 2017, causing Alabama to rank in the top ten states nationally in irrigated land growth. As irrigated land increases in Alabama, the demand for surface or ground water will increase; therefore, implementation of reliable irrigation scheduling tools will be required to increase water use efficiency. Current methods of irrigation scheduling, such as evapotranspiration and soil sensors, have relatively large data collection and analysis demands, which limit their applicability. The fact that less than 9% of Alabama farmers irrigate using some type of sensor-based device (USDA, 2018) helps to explain associated negative impacts of over- or under-irrigation on farm profitability.

Submitted for review in January 2020 as manuscript number NRES 13912; approved for publication as a Research Article and as part of the National Irrigation Symposium 2020 Collection by the Natural Resources & Environmental Systems Community of ASABE in May 2020.

Mention of company or trade names is for description only and does not imply endorsement by the USDA. The USDA is an equal opportunity provider and employer.

The authors are **Bruno P. Lena,** Postdoctoral Fellow, and **Brenda V. Ortiz,** Professor and Extension Specialist, Department of Crop, Soil, and Environmental Sciences, Auburn University, Auburn, Alabama; **Andres F. Jiménez-López,** Professor, Department of Mathematics and Physics, Universidad de los Llanos, Villavicencio, Colombia; **Álvaro Sanz-Sáez,** Assistant Professor, Department of Crop, Soil, and Environmental Sciences, Auburn University, Auburn, Alabama; **Susan A. O'Shaughnessy,** Research Agricultural Engineer, USDA-ARS Conservation and Production Research Laboratory, Bushland, Texas; **Mary K. Durstock,** Graduate Student, Department of Crop, Soil, and Environmental Sciences, Auburn University, Auburn, Alabama; **Greg Pate,** Director, E.V. Smith Research Center, Auburn University, Shorter, Alabama. **Corresponding author:** Bruno P. Lena, 201 Funchess Hall, Auburn University, Auburn, AL 36849; phone: 334-610-5704; e-mail: bzp0043@auburn.edu.

The theoretical crop water stress index (CWSI) (Idso et al., 1981; Jackson et al., 1988) and the temperature-time threshold (TTT) (Wanjura et al., 1992, 1995) have been evaluated as irrigation scheduling methods on multiple crops with promising results (O'Shaughnessy and Evett, 2010; Bockhold et al., 2011; O'Shaughnessy et al., 2012). These methods use an infrared thermometer (IRT) to measure canopy temperature, which is later transformed into indices to indirectly determine plant water stress and subsequently schedule irrigation (O'Shaughnessy et al., 2017). Canopy temperature sensing has an advantage over other methods in its non-destructive nature and comparative low cost to estimate plant water status (DeJonge et al., 2015). Empirical CWSI uses the difference between canopy (T_c) and air (T_a) temperature (i.e., $T_c - T_a$) as a function of vapor pressure deficit (VPD) for its lower limit (Idso et al., 1981). The upper limit is a fixed value of canopy air temperature difference obtained according to crop characteristics and local weather conditions. The TTT method signals plant water stress when canopy temperature is measured above a pre-established temperature threshold for a pre-established period of time over 24 h (Wanjura et al., 1992, 1995). For example, daily corn canopy temperatures above 28°C for more than 240 min are commonly used as a corn water stress indicator (Wanjura et al., 1992).

The use of CWSI and TTT as irrigation scheduling tools has been investigated for many crops in the Southern High Plains region. Using TTT to automatically irrigate soybeans, Peters and Evett (2008) did not find statistically significant yield differences between automated TTT-based and manual irrigation scheduling methods. The authors reported that an automated irrigation system using IRTs mounted on the center pivot can save farmers time in the irrigation decision-making process. Similarly, Evett et al. (2002), using a subsurface drip irrigation system, found comparable or larger corn yields with automated TTT-based irrigation scheduling compared to manual irrigation. They indicated that the TTT-based method resulted in larger water use efficiency (WUE) and irrigation water use efficiency (IWUE). This finding suggests that the TTT method could be a good tool for detecting early plant water stress, thus avoiding yield losses by triggering timely irrigation events. In a study evaluating the implementation of CWSI and TTT algorithms for an automated irrigation scheduling system applied to long- and short-season sorghum, O'Shaughnessy et al. (2012) found that automated irrigated treatments based on CWSI and TTT did not differ statistically from the manual irrigated treatment. Researchers in the High Plains region have also investigated the use of CWSI or TTT as irrigation scheduling tools for corn (Irmak et al., 2000; Lamm and Aiken, 2008; Taghvaeian et al., 2012; Fattahi et al., 2018). All of those studies were conducted in arid and/or semi-arid regions.

Currently, the few farmers in the southeastern U.S. who use irrigation scheduling methods prefer easy-to-use irrigation scheduling tools. Therefore, the use of canopy temperature sensors on an automated moving irrigation system could be an attractive irrigation scheduling tool. The lack of evaluation of this method in humid environments certainly limits its wide adoption. It is also known that upper and lower empirical CWSI baselines are not transferable to different climate regions because they depend on local environmental, soil, and crop characteristics (Alves and Pereira, 2000). Even though Payero and Irmak (2006) attempted to generate variable lower and upper CWSI baselines using weather and canopy data, they emphasized that these equations should be locally calibrated to enhance the successful determination of CWSI for irrigation scheduling. Additionally, Wanjura and Upchurch (1997) found that high relative humidity, prevalent in humid locations, can limit leaf transpiration and increase T_c even with adequate soil water availability. To overcome this issue, they suggested adding a limiting relative humidity (LRH) algorithm to exclude false positive signals of plant water stress by the TTT method. Therefore, an evaluation of empirical CWSI and TTT methods as potential irrigation scheduling tools is necessary for corn in humid environments such as the southeastern U.S. The main objective of this study was to evaluate the sensitivity of CWSI and TTT as irrigation signaling methods for corn growing in a humid environment in the southeastern U.S. The evaluation was done by measuring corn canopy temperature changes under three irrigation levels (100%, 66%, and 33% soil water replenishment to field capacity) established using data from soil water content sensors during the 2018 and 2019 growing seasons. A complementary objective was to develop the lower CWSI baseline from fully watered corn plants for implementation of the CWSI irrigation scheduling method in a humid region.

Materials and Methods

Experimental Field Description

The study was carried out at the E.V. Smith Research Center in Shorter, Alabama (32° 26′ 15″ N, 85° 54′ 57″ W, and 32 m above sea level) in the 2018 and 2019 growing seasons. The location's climate is classified as subtropical humid (Cfa) according to Kottek et al. (2006) with mean high and low temperatures of 24.3°C and 11.7°C, respectively, and accumulated annual rainfall of 1200 mm (http://awis.aumesonet.com/). Agrometeorological parameters were collected at 30 min intervals using a Vantage Pro 2 Plus weather station (model 6163, Davis Instruments, Hayward, Cal.) located about 1500 m east of the experimental area. The same corn hybrid (Dekalb DKC62-08, Bayer Corp., Whippany, N.J.) was cultivated in both years. The hybrid is classified as having very good drought tolerance and has a maturity rating of 112 days. Planting, emergence dates, and main agronomic practices are given in table 1. Corn was planted in concentric rows in 2018 and in straight rows in 2019, at 0.76 m row spacing and a population density of 88,920 seeds ha^{-1}. Herbicide was applied three times during the growing season, as shown in table 1.

Soil texture, soil bulk density, and soil water retention curves (SWRC) were determined from five locations across the experimental area (table 2). At each location, the above properties were measured at soil depths of 0.15, 0.3, and 0.6 m. Percentage by mass of sand, clay, and silt were determined by a commercial soil laboratory (Water Agricultural Laboratories, Camilla, Ga.). Saturated undisturbed soil cores

Table 1. Main agronomic practices, fertilizer rates, and application dates during the 2018 and 2019 seasons.

Practice	2018 Season	2019 Season
Planting	13 April	2 April
Emergence	17 April	8 April
Irrigation events	28 and 30 June; 7, 13, 29, 24, 27, 30 July; 7 August	23, 26, 30 May; 3, 14, 25, 26 June; 1, 5, 11, 12 July
Fertilizer at planting	67 kg N ha^{-1}, 67 kg P ha^{-1}, 67 kg K ha^{-1}	67 kg N ha^{-1}, 67 kg P ha^{-1}, 67 kg K ha^{-1}
Fertilizer during season[a]	11 May and 4 June: 105 kg N ha^{-1}, 19 kg S ha^{-1}	7 and 13 May: 105 kg N ha^{-1}, 19 kg S ha^{-1}
Herbicide applications	15 March: 0.55 kg ha^{-1} paraquat dichloride (1,1′-dimethyl-4,4-bipyridinium dichloride). 3 April: 1.17 kg ha^{-1} S-metolachlor + 1.17 kg ha^{-1} glyphosate, N-(phosphonomethyl)glycine + 0.11 kg ha^{-1} mesotrione + 1.1 kg ha^{-1} 2-chloro-4-ethylamino-6-isopropylamino-s-triazine. 15 May: 0.4 kg ha^{-1} N-(phosphonomethyl)glycine + 1.1 kg ha^{-1} 2-chloro-4-ethylamino-6-isopropylamino-s-triazine.	8 March: 0.4 kg ha^{-1} N-(phosphonomethyl)glycine. 11 April: 0.4 kg ha^{-1} N-(phosphonomethyl)glycine + 1.1 kg ha^{-1} 2-chloro-4-ethylamino-6-isopropylamino-s-triazine. 9 May: 1.17 kg ha^{-1} S-metolachlor + 1.17 kg ha^{-1} glyphosate, N-(phosphonomethyl)glycine + 0.11 kg ha^{-1} mesotrione + 1.1 kg ha^{-1} 2-chloro-4-ethylamino-6-isopropylamino-s-triazine.
Harvest	14 September	31 August

[a] Side-dressing liquid application.

Table 2. Sand, clay, and silt contents, soil type, soil family, volumetric water content at field capacity (θ_{FC}), permanent wilting point (θ_{PWP}), and plant-available water (θ_{PAW}), and bulk density (ρ) at five locations throughout the experimental field.

Location[a]	Sand (%)	Clay (%)	Silt (%)	Soil Type	Soil Family	θ_{FC} ($cm^3\ cm^{-3}$)	θ_{PWP} ($cm^3\ cm^{-3}$)	θ_{PAW} ($cm^3\ cm^{-3}$)	ρ ($g\ cm^{-3}$)
1	46.0	33.7	20.3	Sandy clay loam	Fine-loamy, siliceous, semiactive, thermic Typic Hapludults	0.33	0.20	0.13	1.61
2	79.1	13.9	7.1	Sandy loam	Fine-loamy, mixed, semiactive, thermic Aquic Hapludults	0.19	0.12	0.07	1.77
3	35.9	44.4	19.7	Clay	Fine-loamy, mixed, semiactive, thermic Aquic Hapludults	0.40	0.25	0.15	1.49
4	14.7	57.3	28.0	Clay	Fine-loamy, mixed, semiactive, thermic Aquic Hapludults	0.41	0.28	0.13	1.43
5	27.7	40.3	32.0	Clay	Fine-loamy, siliceous, semiactive, thermic Typic Hapludults	0.34	0.20	0.14	1.53

[a] Locations in the experimental field are shown in figure 1. Values for each location are means of the 0.15, 0.3, and 0.6 m soil depths.

were placed on a hydraulic property analyzer (HYPROP 2, Meter Group, Pullman, Wash.) to determine the relationship between volumetric soil water content (VWC) and soil matric potential (Shokrana and Ghane, 2020). The soil matric potential of saturated undisturbed cores, as evaluated using the hydraulic property analyzer, ranged from 0 to 0.08 MPa. In addition, a dew point hygrometer (WP4C PotentiaMeter, Meter Group) was used to determine the VWC versus soil matric potential relationship at 0.63, 1.5, and 3.3 MPa using disturbed soil samples. The data collected with the hydraulic property analyzer and dew point hygrometer were input to HYPROP-FIT software (ver. 4.1.0.0, Meter Group, http://library.metergroup.com/Manuals/UMS/HYPROP-FIT_Manual.pdf). SWRCs were generated by the traditional unconstrained van Genuchten model (van Genuchten, 1980). VWC at field capacity (FC) was obtained at a soil matric potential of 0.033 MPa for locations 1, 3, 4, and 5, and at 0.01 MPa for location 2. Permanent wilting point (PWP) was obtained at a soil matric potential of 1.5 MPa for all locations. Soil bulk density was calculated as the weight of dry soil (oven-dried at 105°C until constant weight) per unit of volume using undisturbed soil cores.

The experiment was conducted on a field irrigated by a seven-span half-circle 30 ha center pivot irrigation system (model 7000, Valmont Industries, Valley, Neb.) with a lateral length of 434 m. The center pivot operated at a flow of 181.7 $m^3\ h^{-1}$ and a line pressure at the pivot point of 0.241 MPa. The system had a middle-elevation spray application (MESA) sprinkler package equipped with pressure regulators rated at 0.103 MPa. The pivot was retrofitted with a variable-rate irrigation (VRI) system with solenoid valves to control the water application over each half span. The group of sprinklers within each half span (~31 m) represent a grid of 2° arc, for which a single irrigation rate could be prescribed. A John Deere (JD) 9450 combine with a JD 606C six-row header, and a JD 9560 STS combine with a JD 948 six-row header were used for harvest in the 2018 and 2019 seasons, respectively.

TREATMENTS AND IRRIGATION

Full and limited irrigation treatments (T) were established as 100% soil water replenishment to FC (T_{100}), 66% replenishment of the T_{100} rate (T_{66}), and 33% replenishment of the T_{100} rate (T_{33}). Figure 1 shows the layout of the 2018 and 2019 experimental treatment plots. In 2018, the experiment was conducted in arc-wise plots under the fifth span of the center pivot. In 2019, the study was conducted under the third to seventh spans on the west side of the pivot field. A randomized complete block design was used with three treatments and four replications in 2018 (12 plots) and six replications in 2019 (18 plots). The average plot size in 2018 was 3590 m^2. In 2019, the plots were arranged so that the inner plots were wider than the outer plots to reduce plot size variability. As a result, each plot size was 3600 ±70 m^2. In 2018, blocks of three plots each were arranged side by side. In 2019, blocks were arranged so that the three plots were kept as close as possible within a sector.

VWC in the root zone was determined using a time domain reflectometer (TDR-315L, Acclima, Meridian, Ida.) and a capacitance-type soil water sensor (ECH_2O EC-5, Meter Group). In 2018, sensors were installed on 21 May and removed on 30 August, while in 2019 sensors were installed on 23 April and removed on 5 August. VWC data collection

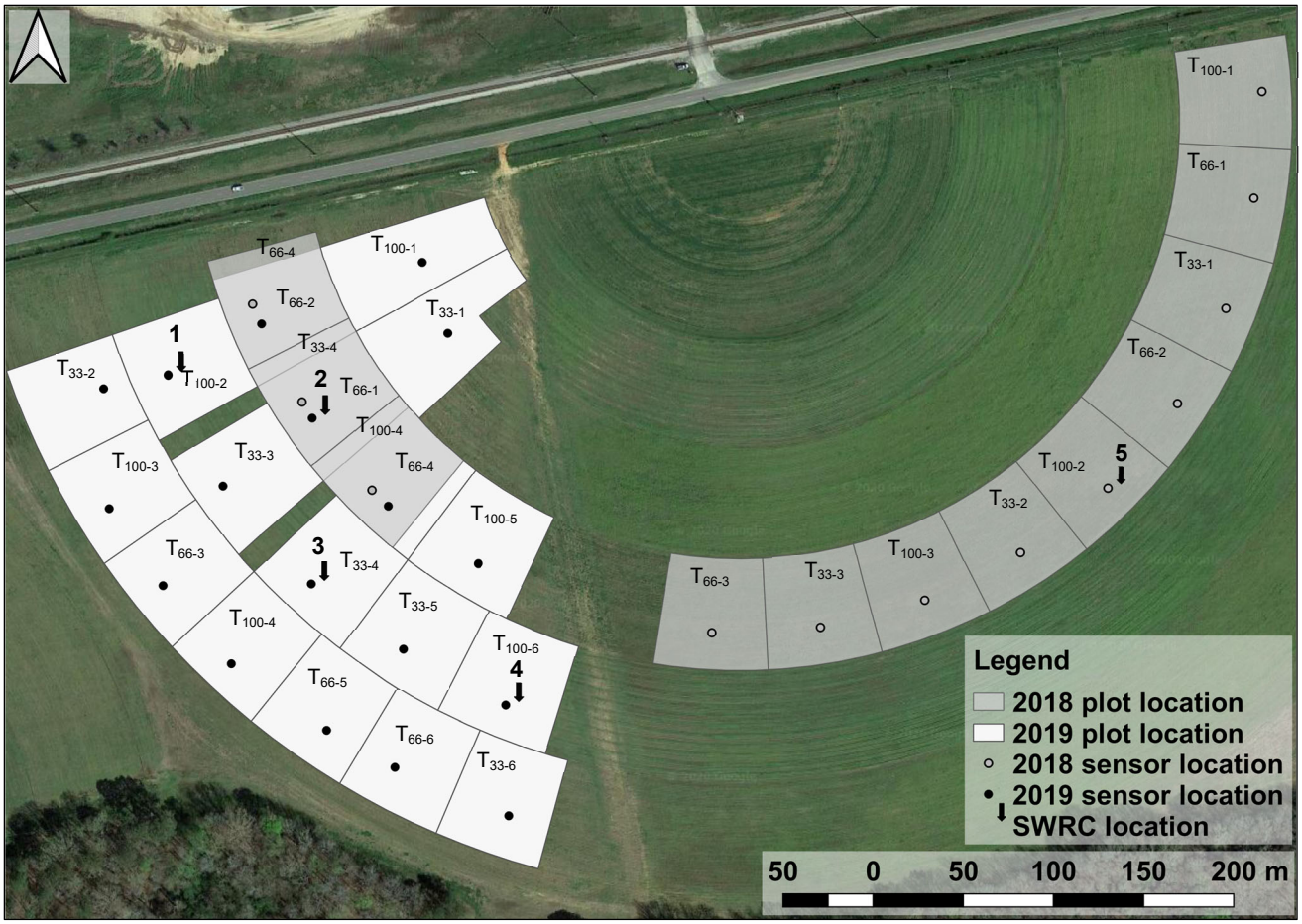

Figure 1. Experiment layout in 2018 and 2019 seasons with irrigation treatments amounts of 33% (T_{33}), 66% (T_{66}), and 100% (T_{100}) of water replenishment to field capacity, sensor location (soil sensors and infrared canopy temperature sensors), and soil sampling location (1 to 5) where soil properties and soil water retention curves (SWRC) were determined. Numbers after treatment code ($T_{100\text{-}n}$) represent replications from 1 to 4 in the 2018 season and from 1 to 6 in the 2019 season.

started on the same day as sensor installation. In both growing seasons, VWC changes in all T_{100} treatments (except for replication 1 in 2018) were assessed using TDR-315L and EC-5 sensors installed at 0.15, 0.3, and 0.6 m soil depths. VWC for the T_{66} and T_{33} treatments was assessed using only EC-5 sensors installed at the same soil depths as the T_{100} treatments. In 2018, an additional TDR-315L sensor was installed at a depth of 0.48 m in the T_{100} treatments. Sensors were installed in a 0.2 m diameter and 0.65 m depth pit opened with an engine-powered auger (fig. 2). The inner wall of the pit was located about 0.05 m from the crop row to prevent damaging the plant roots. All sensors were installed horizontally and at a 45° angle relative to the crop row (fig. 2). In the T_{100} treatments, the TDR-315L and EC-5 sensors were installed in the same pit in opposite directions, forming a 90° angle between them (fig. 2). Dataloggers (Aquatrac, AgSense, Valmont Industries, Inc., Huron, S.D., and model Em50, Meter Group) were used to record and store VWC values at 30 min intervals. The Aquatrac datalogger was used for TDR-315L sensors, and the Em50 datalogger was used for EC-5 sensors. VWC data collection started on 21 May in 2018 and on 28 April in 2019.

Irrigation rates were determined based on the amount of water needed to replenish soil water to FC to a depth of 0.6 m using VWC data from the TDR-315L sensors in the T_{100} treatment. When soil water depletion from at least one of the T_{100} treatments reached 50% of plant-available water (PAW), irrigation was applied for all treatments. The irrigation rate was calculated individually for each experimental block based on the T_{100} treatment. For the T_{66} and T_{33} treatments, irrigation rate was calculated as 66% and 33% of the rate calculated for the T_{100} treatment, respectively. Soil water depletion (SWD, m) was calculated by summing the depletion at each soil layer, using data from four TDR-315L sensors in 2018 and three TDR-315L sensors in 2019:

$$\mathrm{SWD} = \sum_{d=1}^{n} x_d \left(\frac{\theta_{FCd} - \theta_{vd}}{\theta_{FCd} - \theta_{PWPd}} \right) \quad (1)$$

where

n = number of sensors installed

x_d = thickness of soil layer (m) with midpoint at depth d

θ_{vd} = measured volumetric water content ($cm^3\ cm^{-3}$)

θ_{FCd} = measured volumetric water content at field capacity ($cm^3\ cm^{-3}$)

θ_{PWPd} = measured volumetric water content at permanent wilting point ($cm^3\ cm^{-3}$).

The percentage of SWD was calculated as SWD = 100 × SWD / SWD_{max}, where SWD_{max} = 0.6 m. Once irrigation was

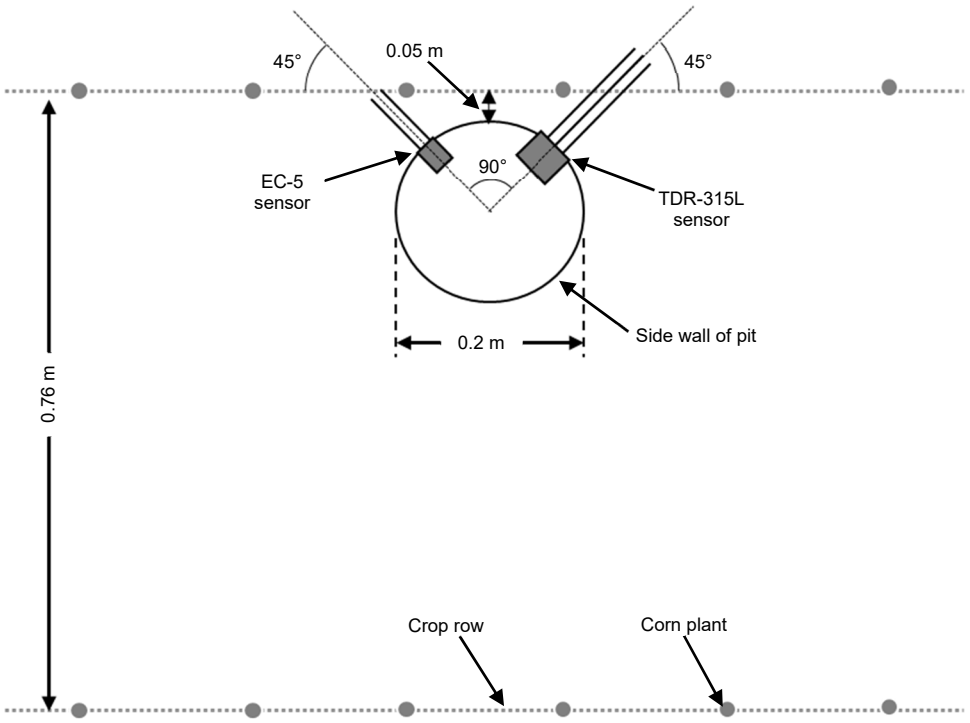

Figure 2. Plan schematic of TDR-315L and EC-5 sensors installed in each experimental plot.

required (based on 50% depletion from PAW threshold) and the amounts were calculated, the irrigation prescription map was generated using Valley VRI (model 8.55, Valmont Industries, Valley, Neb.) and uploaded remotely to the Valley Pro2 panel located at the pivot point.

CANOPY TEMPERATURE, CWSI, AND TTT

Canopy temperature data were recorded with wireless IRT sensors (SapIP-IRT, Dynamax, Houston, Tex.) installed on a stationary mast in each experimental plot (fig. 3). The IRT was designed with a 20° field of view, accuracy of ±0.5°C, and did not require sensor calibration. Canopy temperature was recorded every 10 s and averaged every 30 min to match the weather station data interval. Admittedly, a 30 min average reduces the resolution of the data compared to previous studies (Wanjura et al., 1992; Peters and Evett, 2008). However, the main objective of this research was to evaluate how canopy temperature data and thermal stress indices (CWSI and TTT) relate to different soil water based irrigation regimes and to assess their applicability as potential irrigation signaling tools. Two router modules (SAPIP-REP24-ZB, Dynamax) were used to transmit data from the IRTs to the datalogging unit (IRT-SALH, Infrared Temperature Stress Accumulator/Logger and Host, Dynamax). Data were downloaded on a weekly basis from the coordinator using a personal computer via Wi-Fi connection. A 2 W solar panel facing southwest was used with each IRT to recharge the internal batteries. A 12 V battery along with a 10 W and 30 W solar panel were used to power each router module and datalogging unit, respectively.

In each experimental plot, a single IRT sensor was installed between two corn plants, around the V5 vegetative growth stage (five leaves with visible collar; Abendroth et al., 2011). IRT data collection started on 13 May 2018 and 7 May 2019, which corresponded to the V7 vegetative growth stage (seven leaves with visible collar, fig. 3a). IRTs were installed 1 m above the canopy in the same crop row and 1.5 m from soil water sensors (fig. 3b). The benefit of maintaining a height of 1 m above the canopy is to gain a relatively large surface area for temperature measurement. Each IRT sensor was aimed over the crop row for the entire growing season. The sensor view angle was kept at 90° (facing the crop row) from the V7 to V10 vegetative growth stages and changed to a view angle of 45° after the V10 vegetative growth stage until plants reached R6 (fig. 3b). While soil background radiation may not be entirely eliminated, the combined factors of a field of view of 20°, the IRT angled at 45° from 90°, and the IRT height at 1 m above the canopy helped minimize soil background effects, especially as leaf area increased during the season.

The empirical CWSI was calculated as follows (Idso et al., 1981):

$$\mathrm{CWSI} = \frac{(T_c - T_a) - (T_c - T_a)_{lb}}{(T_c - T_a)_{ub} - (T_c - T_a)_{lb}} \quad (2)$$

where

$(T_c - T_a)$ = difference between canopy temperature (determined with the IRT) and air temperature (determined at the weather station)

$(T_c - T_a)_{lb}$ = lower CWSI baseline for fully watered crop

$(T_c - T_a)_{ub}$ = upper CWSI baseline that represents fully stressed plants for a given VPD.

The lower (non-stressed) CWSI baseline ($CWSI_{LB}$) was generated for the 2018 and 2019 seasons using IRT data from the T_{100} treatments because they were assumed to be non-stressed plants (Idso et al., 1981). IRT data used for the calculation was selected using the following considerations:

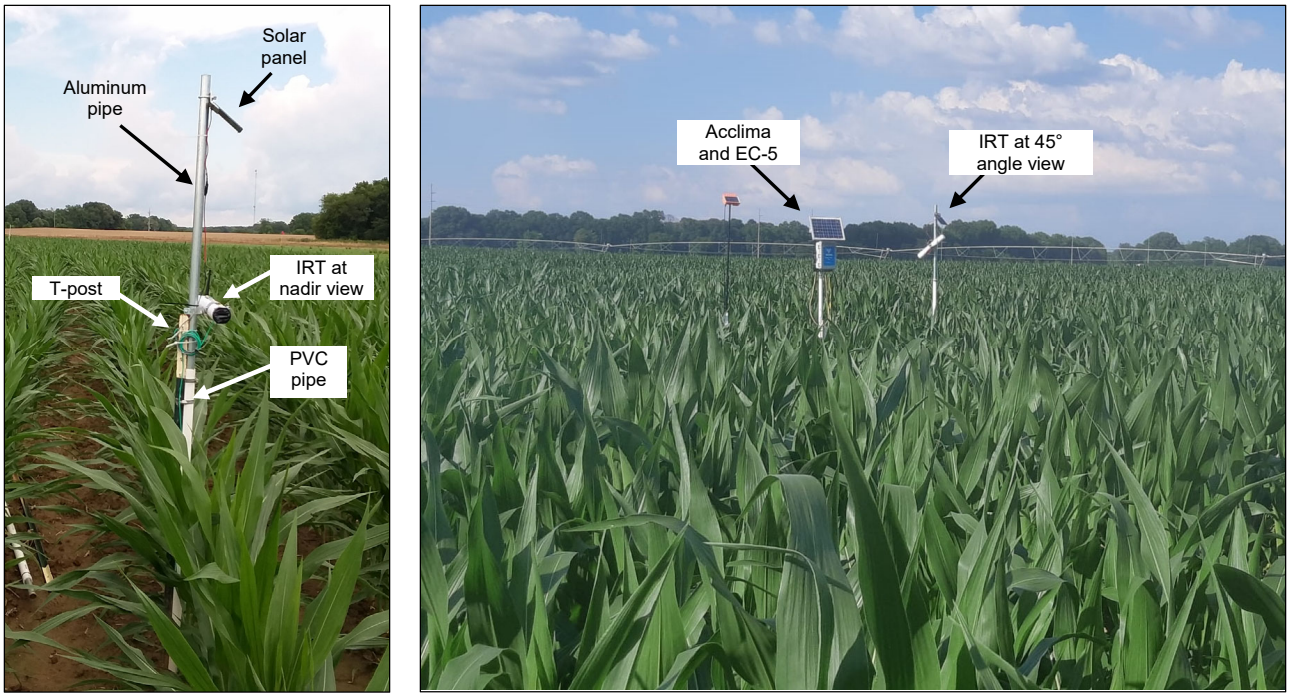

(a) Plants at V7 (b) Plants at V10

Figure 3. IRT support system details at (a) nadir view and (b) 45° angle view along with soil-water based sensors (V7 = vegetative grown state with seven open collars; V10 = vegetative grown state with ten open collars(.

(1) IRT data during the period after irrigation (or precipitation) until soil water status reached 50% depletion of PAW (estimated using TDR-315L data), and (2) data during clear sky conditions and when solar radiation was greater than 750 W m^{-2} s^{-1}. Consequently, IRT data from early in the morning, late in the afternoon, nighttime, and cloudy conditions were not included. Because the largest VPD values were observed around 1500 h on most days analyzed, mean values of T_c, T_a, and VPD from 1300 to 1700 h were used to determine the lower CWSI baseline by simple linear regression between ($T_c - T_a$) and VPD. A constant value of 4°C for corn was used for the upper CWSI baseline [$(T_c - T_a)_{ub}$]. This value was selected as midway between the value of 3°C reported by Shanahan and Nielsen (1987) and Nielsen and Gardner (1987) and the value of 5°C reported by Steele et al. (1994).

For evaluation of TTT as an irrigation signaling tool for corn, a temperature threshold of 28°C and a time threshold of 240 min were used, as described by Wanjura et al. (1992). Therefore, for every 30 min that the canopy temperature was >28°C, 30 min of time was accumulated. Additionally, the limiting relative humidity (LRH) algorithm of Wanjura and Upchurch (1997) was applied to account for days in which relative humidity limited leaf transpiration. The total amount of days that irrigation was signaled using the TTT method when the LRH algorithm was applied was compared to when the LRH algorithm was not applied.

Physiological Parameters

In 2019, stomatal conductance (g_s) and photosynthesis (A) were measured between 1000 h and 1500 h using two infrared gas analyzers (LI-6400XT, LI-COR, Lincoln, Neb.). Readings were taken one day before irrigation events on 26 and 30 May, 14 and 25 June, and 11 July 2019 coinciding, respectively, with corn growth stages V12, VT, R2, R3, and R5. Measurements taken one day before irrigation demonstrated the greatest differences in physiological parameters among the irrigation treatments (Irmak et al., 2000). The equipment was first calibrated outside the corn field, with the chamber light intensity and temperature matched with environmental conditions prior to initiating measurement (~1100 h). The relative humidity in the chamber was maintained at 60% to 70% using the water scrub option available in the infrared gas analyzer when the humidity went above the 70% limit. Two readings per experimental plot were taken from the leaf above the ear with fully opened collar. To maintain repeatable measurements, the LI6400 was zeroed every four measurements (15 to 20 min). Readings were taken from plants on the next crop row and 1 m behind where the IRTs where installed to avoid interference with canopy temperature readings.

Statistical Analysis

All statistical analyses were conducted using R software (R Core Team, 2019). The two linear regressions of ($T_c - T_a$) versus VPD for study years 2018 and 2019 were tested for differences in slope (VPD:year) and intercept (year) through an analysis of variance (ANOVA). Mean difference between CWSI calculated with a $CWSI_{LB}$ developed in a humid region as well as those developed in desert, semiarid, and subhumid regions were tested using paired-sample Student t-tests. The regression model of the relationship between ($T_c - T_a$) and g_s and calculated CWSI versus g_s was transformed from non-linear to linear regression using log-transformation, with the resulting slope tested using ANOVA. Seasonal mean measurements of CWSI, yield, and g_s between irrigation treatments were tested using one-sample Student

t-tests. All statistical analyses were performed at 5% level of probability ($p < 0.05$).

RESULTS AND DISCUSSION

AGROMETEOROLOGICAL PARAMETERS

Monthly averages of agrometeorological variables and monthly total precipitation during the 2018 and 2019 corn seasons are given in table 3. In April, all variables were calculated from planting (13 April 2018 and 2 April 2019) to the end of the month. The same applied to September in 2018; average and total values were calculated from 1 to 14 September (harvest date). Total precipitation in the 2018 season (499 mm) was slightly larger than in 2019 (482 mm), with a difference of only 17 mm between the two seasons. Precipitation amounts were comparable to the 22-year historic averages of 494 and 498 mm, respectively, during the 2018 and 2019 seasons (from 1998 to present, E.V. Smith Research Center HQ, http://awis.aumesonet.com/). Distribution of precipitation is also needed because total precipitation does not provide sufficient information to fully understand crop response to water and irrigation needs. For instance, two precipitation events that occurred on 31 July 2018 (54 mm) and 18 April 2019 (102 mm) increased total seasonal precipitation significantly, but these events occurred when soil water storage was already close to FC (data not shown). Therefore, the majority of the precipitation was likely lost to runoff, deep percolation, or soil evaporation. Furthermore, major precipitation events ranged from 10 to 20 mm d^{-1} in the 2018 season and >20 mm d^{-1} in the 2019 season (data not shown).

Precipitation in the first two months of the field study was 180% larger in the 2019 season compared to the 2018 season. Conversely, from mid-season onward, larger monthly precipitation occurred in the 2018 season (table 3). Total monthly precipitation in April for both study years and in May 2019 were greater than corresponding monthly historical averages. From May through July 2018, monthly precipitation was similar to the historical average, and less than 20 mm in August and September. In 2019, total monthly precipitation in June, July, and August were, respectively, 27%, 66%, and 31% smaller than the 21-year historic average. Precipitation dynamics within the two years of study influenced plant response to irrigation, mainly because irrigation was key to promoting adequate soil water levels when there was a lack of precipitation.

In order to compare and rank precipitation distributions, the Shannon index (Bronikowski and Webb, 1996) was calculated for each month using daily data. The Shannon index varies from 0, representing uneven precipitation distribution, to 1, representing perfectly even precipitation distribution. Larger values of the Shannon index were found in 2018 when compared to the 2019 season, except in April, indicating that precipitation was more evenly distributed in 2018 than in 2019. In general, the 2018 growing season was colder and wetter compared to the 2019 season (table 3).

DEVELOPMENT OF $CWSI_{LB}$

Figure 4 shows 2018 and 2019 linear regression models for canopy-air temperature differential as a function of VPD, obtained using data from the well-watered treatment, T_{100} (Idso et al., 1981). The linear regression was $T_c - T_a = -1.169(VPD)$

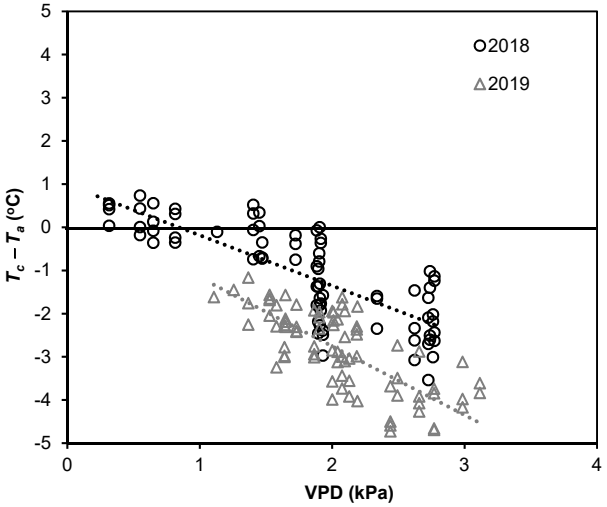

Figure 4. Difference in canopy temperature (T_c) and air temperature (T_a) versus vapor pressure deficit (VPD) for the 2018 and 2019 seasons.

Table 3. Monthly average mean temperature (T_m), mean relative humidity (RH), mean wind speed (u_2), daily mean solar radiation (R_s), average monthly total precipitation (P), historical average monthly total precipitation (P-HA), Shannon index (SI), historical average Shannon index (SI-HA), and 100% irrigation (I) in the 2018 and 2019 seasons.

Season	Month	T_m (°C)	RH (%)	u_2 (m s^{-1})	R_s (MJ m^2 d^{-1})	P (mm)	P-HA mm	SI	SI-HA	I[d] (mm)
2018	April[a]	16.3	73.4	1.3	21.4	73.9	41.3	0.43	0.92	0.0
	May	23.2	79.5	0.9	22.1	92.2	94.2	0.53	0.92	0.0
	June	25.7	83.6	0.8	23.6	106.9	109.0	0.60	0.93	33.2
	July	26.4	83.8	0.8	22.2	121.9	115.0	0.50	0.88	118.1
	August	25.6	86.4	0.7	19.4	82.3	95.6	0.65	0.92	12.7
	September[b]	26.0	84.2	0.8	17.8	21.8	39.0	0.62	0.93	0.0
	Mean or total[c]	23.9	81.8	0.9	21.3	499.1	494.1	0.56	0.92	163.8
2019	April[a]	18.4	79.0	1.1	20.7	182.4	85.1	0.47	0.91	0.0
	May	23.6	80.4	0.7	24.8	114.8	94.2	0.48	0.92	65.6
	June	25.6	81.3	0.8	22.6	80.0	109.0	0.58	0.93	71.1
	July	26.7	80.4	0.7	22.2	39.4	115.0	0.46	0.88	71.1
	August	26.8	80.7	0.7	21.3	65.5	95.6	0.42	0.92	0.0
	Mean or total[c]	24.8	79.4	0.8	22.2	482.1	498.9	0.48	0.92	207.9

[a] April values represent the monthly average mean or total from planting date.
[b] September values represent the mean or total from 1 to 14 September.
[c] Seasonal mean values for T_m, RH, u_2, R_s, SI, and SI-HA, and seasonal total values for P, P-HA, and I.
[d] Values from the T_{100} treatment.

+ 0.983 with r^2 of 0.636 for the 2018 season and $T_c - T_a$ = -1.59(VPD) + 0.433 with r^2 of 0.584 for the 2019 season. For both years, a negative correlation between ($T_c - T_a$) and VPD was found, demonstrating that the difference between $T_c - T_a$ increases as VPD increases. This is in agreement with findings reported by Idso et al. (1981). The above equations indicate that the slope and intercept were smaller in 2019 compared to 2018. Because the study was conducted on the same experimental field but in different growing seasons, the null hypothesis of no difference between both $CWSI_{LB}$ equations was tested. ANOVA testing for differences between coefficients of the linear regression indicated that intercept (year) and slope (VPD:year) were statistically different ($p < 0.05$) (table 4). As seen in the previous section, monthly climatic conditions were different between years, which is an indicator that year-to-year changes in weather conditions should be taken into consideration when using $CWSI_{LB}$. Therefore, the findings from this study suggest that specific $CWSI_{LB}$ equations should be used depending on wetter, average, or dryer seasons with respect to average seasonal values.

Previous studies have also reported different coefficients for $CWSI_{LB}$. Idso (1982) was the first study that mentioned $CWSI_{LB}$ with an intercept and slope of 3.11 and -1.97, respectively. This linear regression was obtained in Arizona, which is classified as a hot desert climate (BWh). In a Mediterranean semiarid climate (Csa), Irmak et al. (2000) developed a $CWSI_{LB}$ equation with an intercept of 1.39 and slope of -0.86. In a humid continental climate (Cfb), Steele et al. (1994) determined an intercept of 2.14 and a slope of -1.97. Irmak et al. (2000) stated that site, climate, and plant characteristics influence $CWSI_{LB}$ linear regression coefficients; therefore, local calibration of $CWSI_{LB}$ is required to enhance the use of an empirical CWSI as an irrigation scheduling tool (Alves and Pereira, 2000; Payero and Irmak, 2006). Differences between these equations influence the estimation of CWSI and subsequent irrigation recommendations. In this study, the potential effects of different equations on CWSI values were evaluated. Figure 5 shows a comparison of daily 2018 and 2019 CWSI values estimated using the $CWSI_{LB}$ generated from this study and the $CWSI_{LB}$ representing desert (Idso, 1982), semiarid (Irmak et al., 2000), and subhumid (Steele et al., 1994) climatic conditions. The proximity of r^2 values to 1 for all linear regression models in figure 5 indicates that the $CWSI_{LB}$ from climates different from this study might be used with satisfactory results to estimate empirical CWSI. However, it is important to note that the large amount of normally distributed data available for this comparison favored larger r^2 values, making identification of CWSI differences difficult using different equations. For example, the expected range of CWSI for fully watered plants lies within 0 to 0.2 (Irmak et al., 2000; Han et al., 2018), and this was the range in which most discrepancies between CWSI values using different $CWSI_{LB}$ equations were found (fig. 5). These discrepancies suggest that CWSI-based irrigation scheduling using different equations could have resulted in delayed or under-irrigation, potentially impacting plant development and yield, especially if water deficiencies occurred during periods of large crop water use.

Results comparing calculated CWSI values using $CWSI_{LB}$ developed in this study for a humid region and CWSI values calculated using $CWSI_{LB}$ developed in other regions (desert, semiarid, and subhumid) are given in table 5. Difference in CWSI means were significant ($p < 0.001$) for all combinations of year and location, except for CWSI generated in 2018 using $CWSI_{LB}$ from a subhumid climate. Results validate the hypothesis that the transferability of $CWSI_{LB}$ from contrasting climates could lead to over- or underestimation of CWSI values, thereby impacting irrigation scheduling. In contrast, similarity between calculated CWSI using $CWSI_{LB}$ from a subhumid environment and the equation derived for Alabama climate conditions in 2018 indi-

Table 4. Analysis of variance results for the 2018 and 2019 seasons.

	df	SS	MS	F	p-Value[a]
VPD	1	160.5	140.39	366.1	<0.001***
Year	1	68.7	81.26	156.8	<0.001***
VPD:year	1	2.3	2.31	5.26	0.023*
Residuals	150	65.8	0.44		

[a] Asterisks indicate significant differences at the (***) 0.001 and (*) 0.05 levels of probability.

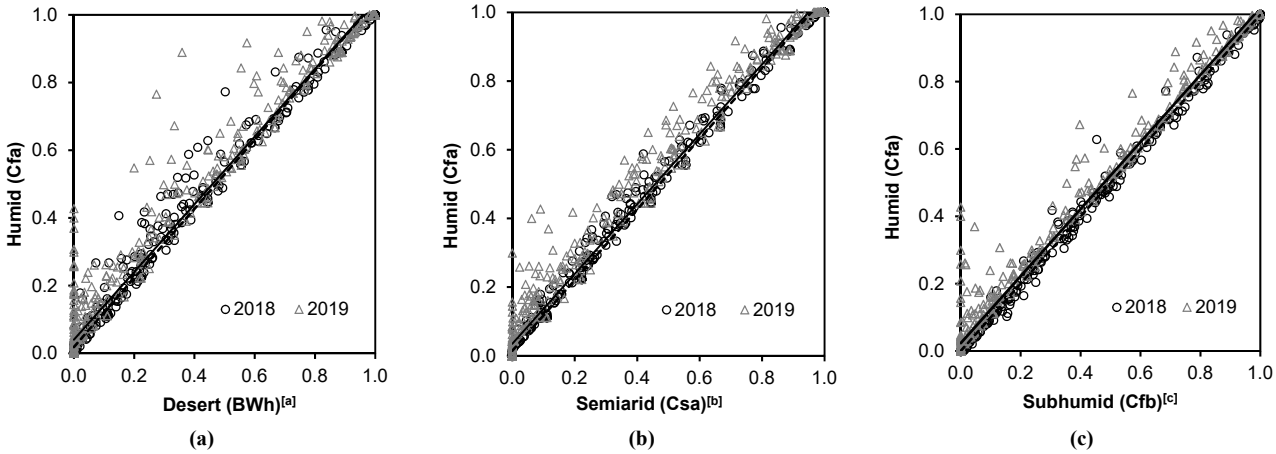

Figure 5. Calculated CWSI using $CWSI_{LB}$ for (a) desert, (b) semiarid, and (c) subhumid climate types for the 2018 and 2019 seasons. Dashed lines and solid lines represent linear regressions for 2018 and 2019, respectively:

[a] For 2018: CWSI(Cfa) = 1.020 × CWSI(BWh) + 0.019 (r^2 = 0.982); for 2019: CWSI(Cfa) = 0.997 × CWSI(BWh) + 0.042 (r^2 = 0.961).

[b] For 2018: CWSI(Cfa) = 1.018 × CWSI(Csa) + 0.015 (r^2 = 0.992); for 2019: CWSI(Cfa) = 1.017 × CWSI(Csa) + 0.034 (r^2 = 0.978).

[c] For 2018: CWSI(Cfa) = 0.999 × CWSI(Cfb) + 0.000 (r^2 = 0.997); for 2019: CWSI(Cfa) = 0.996 × CWSI(Cfb) + 0.024 (r^2 = 0.985).

cates that baselines could be transferrable under specific climate conditions. Further investigation is necessary to evaluate whether $CWSI_{LB}$ can be transferable to climate types that contrast with where it was developed.

Table 5. Paired sample t-test results for daily calculated CWSI using $CWSI_{LB}$ generated in humid (Cfa) and in desert (BWh), semiarid (Csa), and subhumid (Cfb) climate types.[a]

Year	Interaction	t	df	p-Value	Mean Difference
2018	Cfa:BWh	10.35	383	<0.001***	0.023 ±0.005
	Cfa:Csa	14.09	383	<0.001***	0.022 ±0.003
	Cfa:Cfb	-0.13	383	0.89 ns	-0.000 ±0.002
2019	Cfa:BWh	12.94	575	<0.001***	0.042 ±0.006
	Cfa:Csa	16.47	575	<0.001***	0.041 ±0.005
	Cfa:Cfb	10.12	575	<0.001***	0.023 ±0.002

[a] *** = significant at 0.001 level of probability, ns = not significant at 0.05 level of probability, and df = degrees of freedom.

CWSI AND IRRIGATION TREATMENTS

Daily empirical CWSI changes in 2018 and 2019 for all irrigation treatments are presented in figure 6. Missing data were a result of precipitation events or solar radiation below the threshold (750 W m^{-2} s^{-1}). Larger CWSI values were found early and late in the growing season compared to mid-season, although plants were not under water deficit (soil water depletion <30%, data not shown). Early growing season results could be due to the impact on soil background reflectance due to limited canopy cover. Later in the growing season, combined effects of reduced plant transpiration and decreased leaf area index (due to leaf senescence) explain the larger CWSI values. Similar results were reported by other authors (Han et al., 2018), who noted that the use of unadjusted CWSI for corn irrigation scheduling is limited to

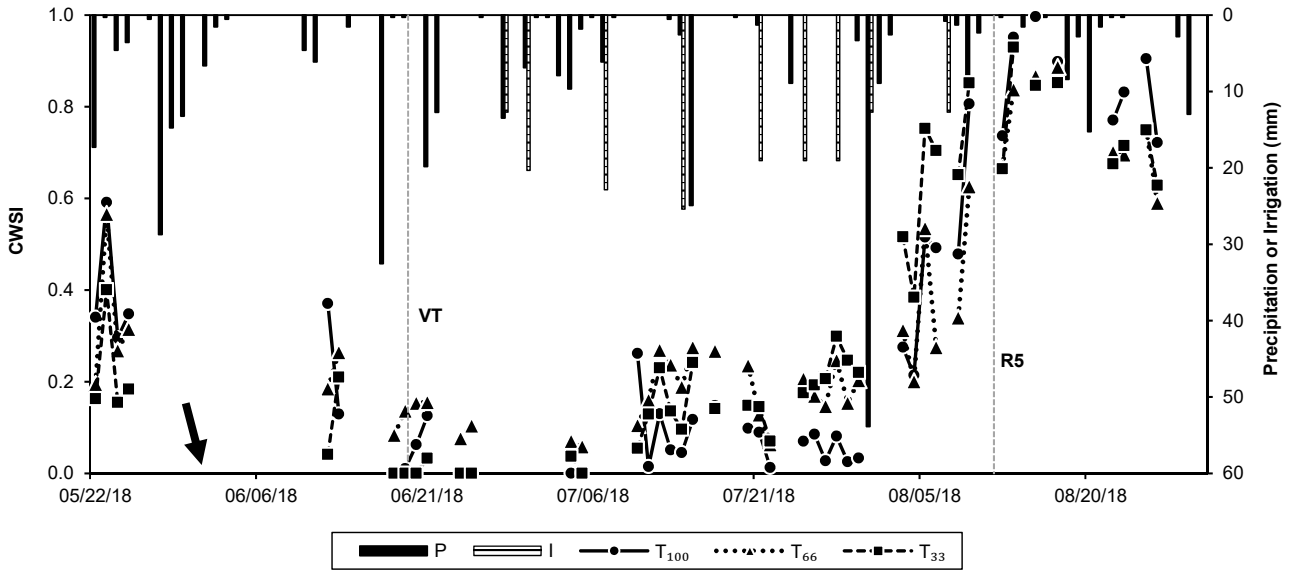

(a)

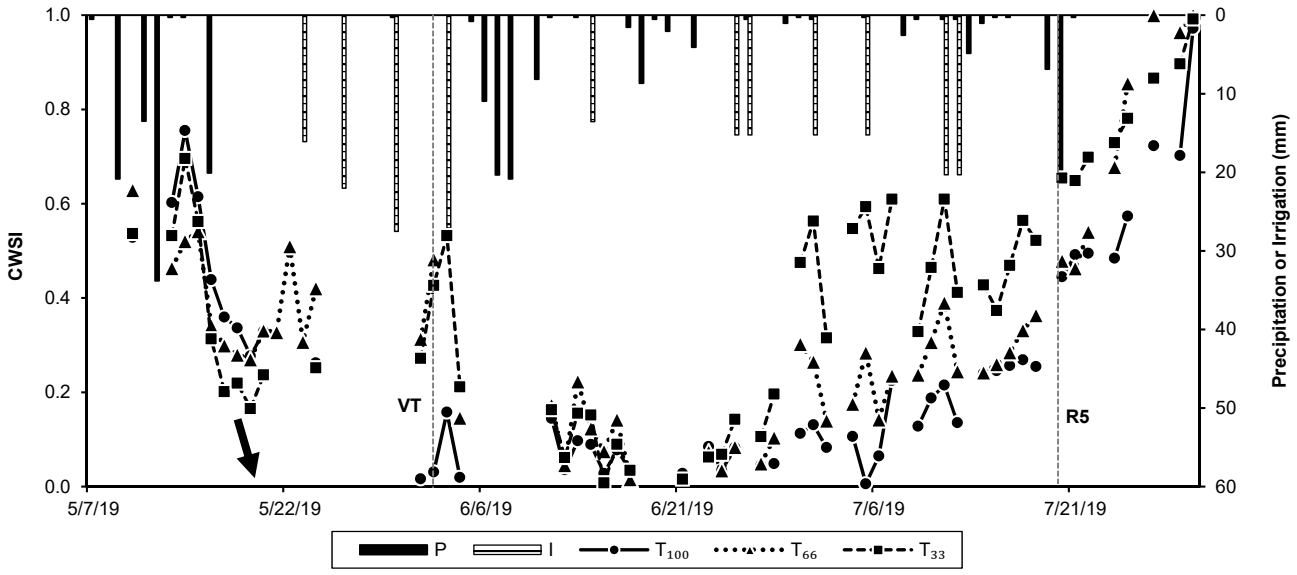

(b)

Figure 6. Crop water stress index (CWSI, dimensionless) for 100% water replenishment to FC (T_{100}), 66% replenishment (T_{66}), and 33% replenishment (T_{33}) treatments, precipitation (P), and irrigation (I) during the (a) 2018 and (b) 2019 seasons. Arrows indicate the date when the IRT view was modified from nadir to 45° angle.

the interval between tasseling (VT) and dent (R5), when full soil coverage by the canopy is anticipated to occur.

As anticipated, an increasing trend in CWSI was observed as soil water was depleted due to crop evapotranspiration in all treatments. Decreased CWSI values after irrigation and precipitation events were similarly observed. Different irrigation amounts also affected daily CWSI values between treatments. For the T_{100} treatment during the VT to R5 growing period in both years, CWSI values were close to or equal to 0, indicating that the plants were fully watered. An inverse trend of increased CWSI was observed in the reduced-irrigation T_{66} and T_{33} treatments. More evenly distributed precipitation in the 2018 season (table 3) resulted in fewer differences in CWSI values between full and limited irrigation treatments, even after irrigation was initiated. For example, when different CWSI values among the treatments were observed on 14 July 2018, a precipitation event of 25 mm on 15 July reduced and almost equalized CWSI in all treatments (fig. 6a). In contrast, in 2019, the lack of precipitation from 22 June to 15 July between the R2 and R5 growth stages (corresponding to greater corn water demand), resulted in substantial separation of CWSI values between T_{100} and treatments T_{66} and T_{33} (fig. 6b).

Overall, the fully irrigated T_{100} treatment resulted in CWSI values below 0.2. This was especially evident in 2019, when precipitation was sparser than in 2018 (table 3). Interestingly, for the T_{66} and T_{33} treatments in both years, CWSI values dropped the day after irrigation, with the largest reductions occurring when pre-irrigation CWSI was >0.4. Corn plants experience greater water stress when CWSI values are >0.2 (Steele et al., 1994; Irmak et al., 2000) and respond quickly even under incremental increases in water availability, as shown in figure 6 for T_{66} and T_{33} (table 3). Similar CWSI response to full irrigation, deficit irrigation, and plant water uptake have been observed for corn (Yazar et al., 1999; Irmak et al., 2000) as well as wheat (Gontia and Tiwari, 2008), soybean (Candogan et al., 2013; Tekelioğlu et al., 2017), grain sorghum (O'Shaughnessy et al., 2012), and cotton (Usman et al., 2009; Ünlü et al., 2011).

No statistical differences ($p > 0.05$) in seasonal mean CWSI (from VT to R5) nor yield across irrigation treatments were found during the 2018 season (table 6). In contrast, the 2019 treatment means for CWSI and yield were significantly different. Smaller CWSI and larger yield values were found in 2019 for T_{100} compared to 2018, with corresponding larger CWSI and smaller yields for the 2019 T_{33} treatment. The absence of drought periods and timely precipitation events in 2018 likely contributed to similar soil water levels between treatments, explaining the lack of difference in yield and seasonal CWSI. In 2019, irrigation was key to maintaining adequate soil water levels during longer drought periods in the T_{100} treatment compared to the limited irrigation treatments. As expected, full irrigation resulted in greater yield and lesser seasonal CWSI. Figure 6b and table 6 show that CWSI values increased as soil water level decreased, suggesting that CWSI could be used as a surrogate method to assess potential crop water stress related to different soil plant-available water levels. The sensitivity of CWSI to the different irrigation levels tested and to changes in the weather conditions observed throughout the growing season shows its potential use in real-time irrigation triggering in the humid subtropical climate of the southeastern U.S.

Table 6. Student t-test results for seasonal mean CWSI and yield for 100% replenishment to FC (T_{100}), 66% replenishment (T_{66}), and 33% replenishment (T_{33}) treatments in 2018 and 2019.[a]

Year	Treatment	Seasonal Mean CWSI[b]	Yield (Mg ha^{-1})
2018	T_{100}	0.19 a	11.47 a
	T_{66}	0.25 a	11.72 a
	T_{33}	0.29 a	10.75 a
2019	T_{100}	0.12 a	13.59 a
	T_{66}	0.21 b	11.79 b
	T_{33}	0.33 c	10.08 c

[a] Values in the same column and the same year followed by the same letter do not differ at 5% probability level.

[b] Value are means of daily CWSI from VT to R5 interval.

CWSI, Yield, and Crop Physiology Assessment

Mean differences in A and g_s between the irrigation treatments are given in table 7. The mean A for fully irrigated plants (T_{100}) was greater and significantly different from the T_{33} treatment mean, but not from T_{66}. The mean g_s for the T_{100} treatment was greater and significantly different from both T_{66} and T_{33}, while the g_s values for T_{33} and T_{66} were not significantly different (table 7). Greater values of g_s and A for T_{100}, when compared with the T_{33} treatment, show the effect of full irrigation to promote plant growth, photosynthesis, and carbon fixation, resulting in greater yield. These results help explain the differences between seasonal CWSI and yield in the 2019 season (table 6), when plants kept under adequate water levels throughout the season took full advantage of available water to provide larger yield.

Although many studies have investigated the use of canopy temperature data as an irrigation scheduling tool for corn (Steele et al., 1994; Irmak et al., 2000; Taghvaeian et al., 2012; Fattahi et al., 2018), uncertainties remain regarding the critical value of CWSI at which plants are under water deficit stress and when irrigation should be initiated. Therefore, g_s was measured one day before three irrigation events in all replications and treatments in the 2019 season as a tool to relate physiological parameters with canopy temperature data (fig. 7). Due to experimental constraints, canopy temperature was not recorded from 24 to 30 May 2019, coinciding with the first two measurements of A and g_s. Therefore, the results shown in figure 7 represent physiological measurements for 14 and 25 June and 11 July 2019 only, while the means in table 7 represent the five measurements taken across the entire season.

Negative logarithmic relationships were found between $(T_c - T_a)$ and between g_s and CWSI and g_s, while a positive linear relationship was found between corn grain yield and g_s (fig. 7). At greater values of g_s, it was noted that the plants

Table 7. Student t-test results for mean photosynthesis (A) and stomatal conductance (g_s) from five measurements one day before irrigation in the 100% replenishment to FC (T_{100}), 66% replenishment (T_{66}), and 33% replenishment (T_{33}) treatments.[a]

Treatment	Mean Photosynthesis (A, μmol CO_2 mol^{-1} m^{-2} s^{-1})	Stomatal Conductance (g_s, mol m^{-2} s^{-1})
T_{100}	29.02 a	0.33 a
T_{66}	25.94 ab	0.23 b
T_{33}	23.59 b	0.21 b

[a] Values in the same column followed by the same letter do not differ at 5% probability level.

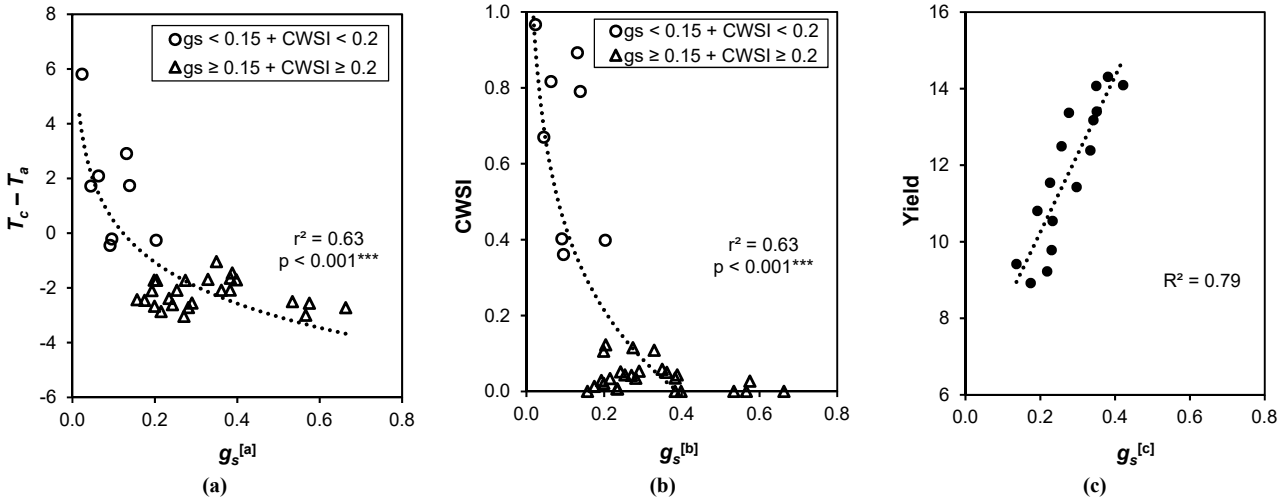

Figure 7. (a) Canopy temperature minus air temperature ($T_c - T_a$, °C) versus stomatal conductance (g_s, mol m^{-2} s^{-1}), (b) crop water stress index (CWSI) versus g_s, and (c) yield (Mg ha^{-1}) versus g_s.

[a] $T_c - T_a$ = -2.18[ln(g_s)] – 4.57 (* = significant at 0.001 level of probability).**

[b] CWSI = -0.32[ln(g_s)] – 0.30 (* = significant at 0.001 level of probability).**

[c] Yield = 20.38(g_s) + 6.17.

were cooler than the air temperature (fig. 7a), and calculated CWSI decreased rapidly before reaching 0 (fig. 7b). In contrast, periods of increased leaf temperature (when plants were hotter than the air temperature) and increased CWSI were observed as g_s decreased, indicating that lack of available water limited leaf transpiration and evaporative cooling. Lesser corn yield values were found under these lesser g_s values, and yield increased linearly as g_s increased. Sabagh et al. (2017) reported a second-degree polynomial function between corn yield and g_s, also indicating that larger yields occurred with larger g_s. In a study investigating the effects of different water levels on several corn growth characteristics, Ma et al. (2018) found that the tipping point of the growth characteristic for stem moisture and leaf moisture content, net photosynthetic rate, and transpiration rate occurred when g_s was <0.15 mol m^{-2} s^{-1}. Based on those studies and the results shown in figure 7, we hypothesize that there is a greater chance that plants suffer stress when g_s is <0.15 mol m^{-2} s^{-1}, which was also found by Cabrera-Bosquet et al. (2009) for a set of tropical maize hybrids cultivated under different water levels. In the current study, most of the CWSI values less than 0.2 (figs. 7a and 7b) occurred when g_s was >0.15 mol m^{-2} s^{-1}. There would be a need to closely track CWSI values as they approach 0.2 so that irrigation events could be triggered. Site-specific evaluation with repeated measurements throughout the season under a wide range of CWSI values is required to identify precise threshold CWSI values at which irrigation should be initiated to prevent yield losses.

Temperature-Time Threshold

Differences between treatments were observed with respect to the time when corn canopy temperature exceeded threshold temperature (CTETT) of 28°C in 2018 and 2019 (figs. 8 and 9). In 2018, seasonal mean daily cumulative time when CTETT, without applying the limiting relative humidity (LRH) algorithm, was 525, 541, and 533 min for the T_{100}, T_{66}, and T_{33} treatments, respectively. In 2019, the corresponding mean daily cumulative time was 464, 484, and 510 min for the same treatments, with no significant differences observed between irrigation treatments ($p < 0.05$). The time threshold of 240 min was exceeded on all 26 days in all treatments in which the TTT method was evaluated in 2018. Similar results were found in the 2019 season; of 33 days evaluated, the time threshold was exceeded on all but three days for the T_{100} treatment and all but two days for the T_{66} and T_{33} treatments. The above results indicate that irrigation would have been triggered for all treatments every day if the TTT method was used to schedule irrigation. This finding demonstrates that the TTT method, when the LRH algorithm is not applied, is not a realistic irrigation scheduling tool for humid areas of the U.S., at least until more research is conducted.

When the LRH algorithm was applied to compensate for high relative humidity, a decrease occurred in the amount of accumulated time when CTETT (figs. 8 and 9). In 2018, seasonal mean daily accumulated time was 92, 99, and 93 min for T_{100}, T_{66}, and T_{33}, respectively. In 2019, the corresponding daily accumulated time was 80, 84, and 93 min for T_{100}, T_{66}, and T_{33}, respectively, with no significant differences between treatments for both years ($p > 0.05$). The above values represent reductions of 82.1% and 82.3% in the accumulated time, respectively, for the 2018 and 2019 seasons, compared with the TTT values when the LRH algorithm was not applied. Although the interval for averaging the TTT was greater than that used by USDA-ARS scientists in Lubbock, Texas (Wanjura et al., 1992, 1995) and Bushland, Texas (Evett et al., 2000), the objective of the current study was to test canopy temperature technology performance for an Alabama climate type. Even using a relatively large temporal resolution of 30 min, it was possible to show that in a climate with sustained high relative humidity (low VPD), it is difficult for a plant to cool itself through transpiration. At the very least, if the TTT method were used, a limiting factor for relative humidity would need to be applied to limit the frequency of irrigation triggers.

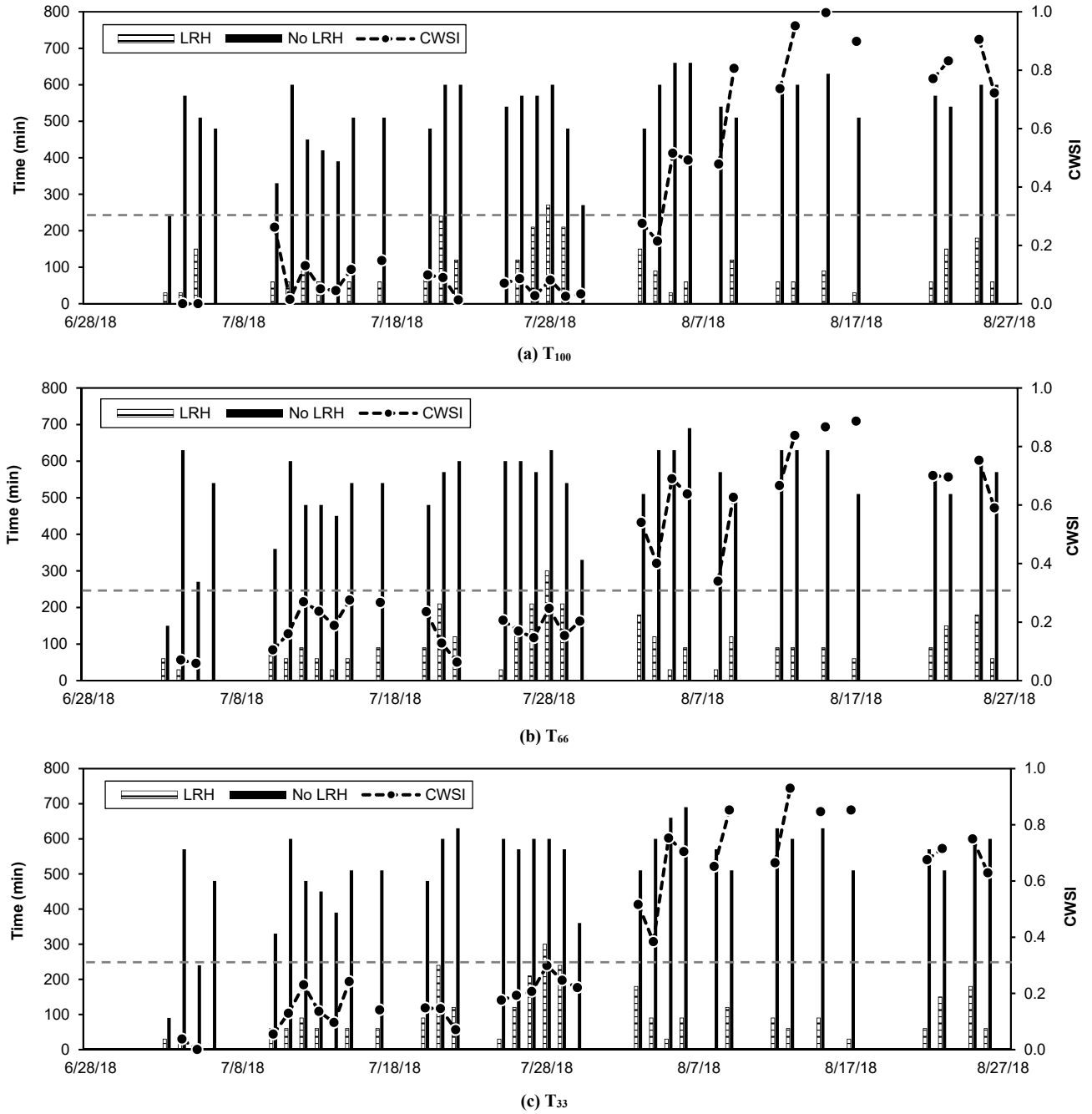

Figure 8. Daily accumulated time when canopy temperature exceeded 28°C and crop water stress index (CWSI) for the (a) 100% of water replenishment to FC (T_{100}), (b) 66% replenishment (T_{66}), and (c) 33% replenishment (T_{33}) treatments during the 2018 season when applying (LRH) and not applying (No LRH) the limiting relative humidity algorithm.

Figure 10 shows the change in T_c and T_a over three days when physiological measurements were taken. When plants were at R2 (14 June 2019), the temperature threshold was not exceeded; therefore, irrigation would have not been triggered whether or not the LRH algorithm was applied. An agreement between g_s values >0.15 mol m^{-2} s^{-1} (well transpiring plants) and no irrigation needed was found. The g_s values observed on 25 June 2019 indicate that the corn plants were fully transpiring in all treatments. The TTT method performed well when LRH was added to the algorithm (irrigation would have not been triggered). In contrast, the TTT method performed poorly when LRH was not included (ac-cumulated time of 490 min, and irrigation was triggered). When the TTT method was evaluated on limited irrigation treatments experiencing water deficit stress (g_s < 0.15 mol m^{-2} s^{-1} on 11 July 2019), the use of the LRH algorithm did not perform well by not triggering irrigation (90 min for both T_{33} and T_{66}, data not shown). For the T_{100} treatment, only 30 min of cumulated time above the threshold temperature was observed when the LRH method was applied, which agreed with the larger g_s values observed (>0.15 mol m^{-2} s^{-1}). Conversely, days when irrigation would have been triggered using the TTT method agreed with stomatal conductance measurements for T_{66} and T_{33} when the

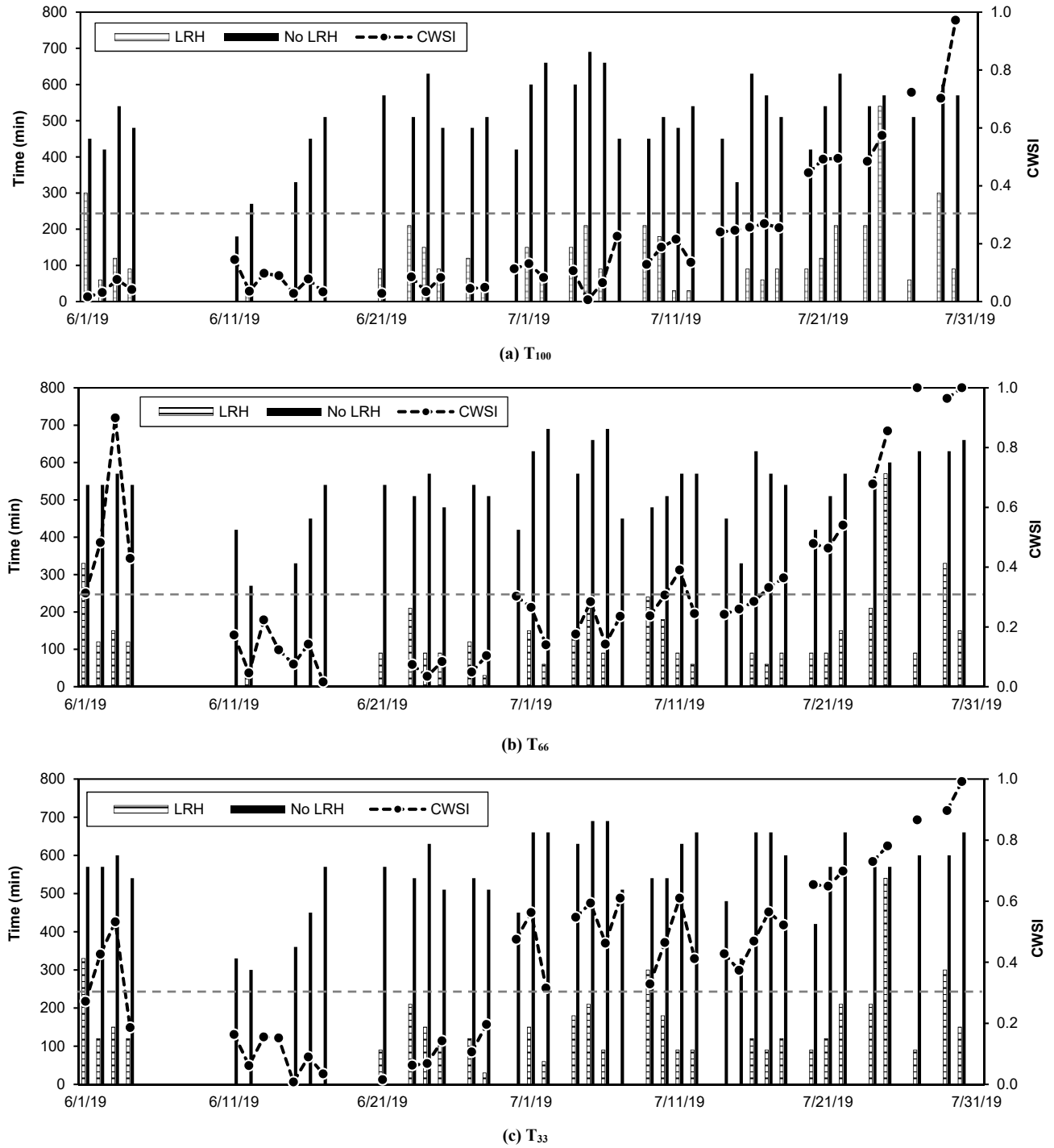

Figure 9. Daily accumulated time when canopy temperature exceeded 28°C and crop water stress index (CWSI) for the (a) 100% of water replenishment to FC (T_{100}), (b) 66% replenishment (T_{66}), and (c) 33% replenishment (T_{33}) treatments during the 2019 season when applying (LRH) and not applying (No LRH) the limiting relative humidity algorithm.

LHR algorithm was not applied but were in disagreement with the T_{100} treatment.

Overall, results from the evaluation of the TTT method with or without the use of the LRH algorithm as an irrigation timing tool in comparison with physiological measurements indicated that the TTT method was inconsistent throughout the season and would not perform well under humid climate conditions. An opportunity remains to more thoroughly investigate this method over different temperature and time thresholds for other crops including cotton (O'Shaughnessy et al., 2010). Measurement of physiological parameters will remain key to identifying plants under water stress, to relate these values with water stress indexes, and to calibrate threshold values to enhance the reliability of the TTT method as an irrigation scheduling tool for humid environments.

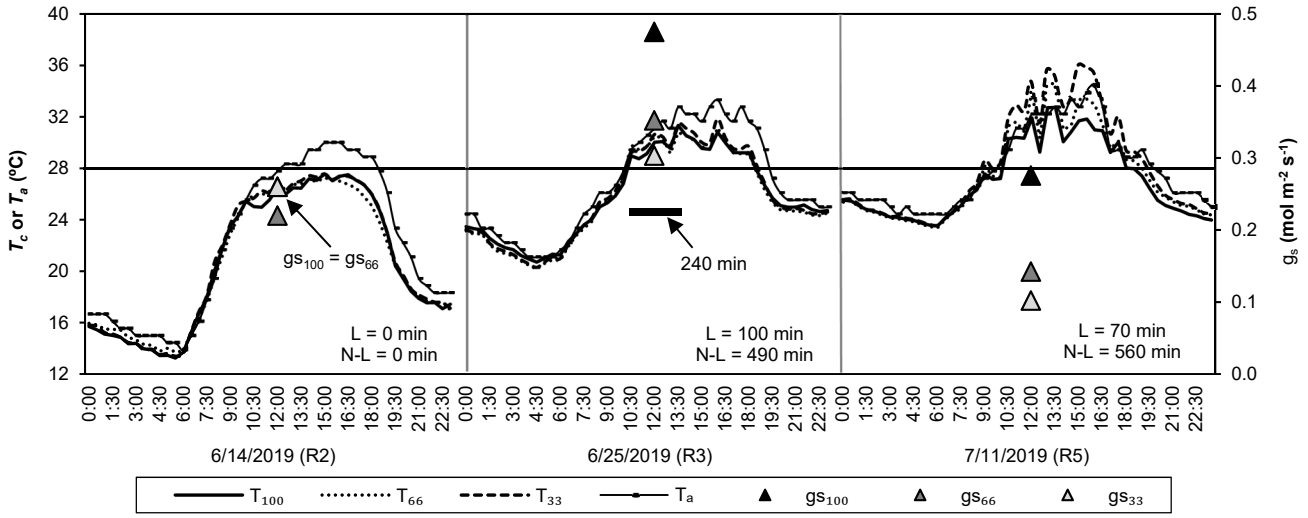

Figure 10. 30 min mean values of canopy (T_c) and air temperature (T_a) for the 100% of water replenishment to FC (T_{100}), 66% replenishment (T_{66}), and 33% replenishment (T_{33}) treatments and stomatal conductance (g_s) for T_{100} (gs_{100}), T_{100} (gs_{66}), and T_{100} (gs_{33}). L and N-L are the average accumulated time for all treatments when the temperature exceeded the 28°C threshold (horizontal line) and when the limiting relative humidity was applied (L) or not applied N-L).

CONCLUSIONS

The use of canopy temperature data as a potential irrigation signaling tool for corn in a humid subtropical climate during the 2018 and 2019 seasons was investigated. Although accumulated seasonal precipitation amounts in the two years of study were comparable with each other and with the historical average, it was found that precipitation was more evenly distributed in 2018 than in 2019. Precipitation distribution influenced plant development, yield, and the CWSI dynamic among irrigation treatments. In 2018, CWSI and yield were similar between the T_{100}, T_{66}, and T_{33} treatments, and this was explained by timely precipitation during the growing season. In comparison, because precipitation was less evenly distributed in 2019, irrigation promoted differences in CWSI and yield values between the irrigation treatments. The T_{100} treatment was observed to have smaller CWSI and larger yield values when compared to the T_{66} and T_{33} treatments. Physiological measurements were compared with CWSI values in an attempt to identify a CWSI threshold value at which plants indicate water stress and irrigation should be initiated. When stomatal conductance was <0.15 mol m^{-2} s^{-1}, most of the CWSI values were >0.2, indicating plant water stress. However, further investigation is recommended to determine an accurate CWSI threshold value for irrigation to prevent corn yield losses. It is also important to emphasize that given inter-annual weather differences, CWSI threshold values may not be constant. The TTT method as an irrigation timing tool (with a temperature threshold of 28°C and a time threshold of 240 min) did not perform well under the site and humid climate conditions evaluated, whether the limiting relative humidity factor was implemented or not. The results of this study indicate the need for further investigation focusing on the calibration of different time and temperature values for humid environments.

ACKNOWLEDGEMENTS

This research was funded by the Alabama Wheat Feed Grain Committee, the Alabama Soil and Water Conservation Committee, Alabama Agricultural Experiment Station, Dynamax Inc., and AU Tiger Day funding. We also would like to recognize Barret Mason, Kyle Stewart, Mary Heron, and Taylor Putman for their collaboration with data collection.

REFERENCES

Abendroth, L. J., Elmore, R. W., Boyer, M. J., & Marlay, S. K. (2011). Corn growth and developlment. PMR 1009. Ames, IA: Iowa State University Extension.

Alves, I., & Pereira, L. S. (2000). Non-water-stressed baselines for irrigation scheduling with infrared thermometers: A new approach. *Irrig. Sci., 19*, 101-106. https://doi.org/10.1007/s002710050007

Bockhold, D. D., Thompson, A. L., Sudduth, K. A., & Henggeler, J. C. (2011). Irrigation scheduling based on crop canopy temperature for humid environments. *Trans. ASABE, 54*(6), 2021-2028. https://doi.org/10.13031/2013.40654

Bronikowski, A., & Webb, C. (1996). Appendix: A critical examination of rainfall variability measures used in behavioral ecology studies. *Behav. Ecol. Sociobiol., 39*(1), 27-30. https://doi.org/10.1007/s002650050263

Cabrera-Bosquet, L, Sánchez, C, & Araus, J. L. (2009). Oxygen isotope enrichment ($\Delta^{18}O$) reflects yield potential and drought resistance in maize. *Plant Cell Environ., 32*(10), 1487-1499. https://doi.org/10.1111/j.1365-3040.2009.02013.x

Candogan, B. N., Sincik, M., Buyukcangaz, H., Demirtas, C., Goksoy, A. T., & Yazgan, S. (2013). Yield, quality, and crop water stress index relationships for deficit-irrigated soybean [*Glycine max* (L.) Merr.] in sub-humid climatic conditions. *Agric. Water Mgmt., 118*, 113-121. https://doi.org/10.1016/j.agwat.2012.11.021

DeJonge, K. C.,Taghvaeian, S., Trout, T. J., & Comas, L. H. (2015). Comparison of canopy temperature-based water stress indices for maize. *Agric. Water Mgmt., 156*, 51-62. https://doi.org/10.1016/j.agwat.2015.03.023

Evett, S. R., Howell, T. A., Scheneider, A. D., Upchurch, D. R., & Wanjura, D. F. (2000). Automatic drip irrigation of corn and soybean. *4th Decennial National Irrigation Symp.* (pp. 401-408). St. Joseph, MI: ASABE.

Evett, S. R., Howell, T. A., Schneider, A. D., Wanjura, D. F., & Upchurch, D. R. (2002). Automatic drip irrigation control regulates water use efficiency. *Intl. Water Irrig., 22*(2), 34-37.

Fattahi, K., Babazedeh, H., Najafi, P., & Sedghi, H. (2018). Scheduling maize irrigation based on crop water stress index (CWSI). *Appl. Ecol. Environ. Res., 16*(6), 7535-7549. https://doi.org/10.15666/aeer/1606_75357549

Gontia, N. K., & Tiwari, K. N. (2008). Development of crop water stress index of wheat crop for scheduling irrigation using infrared thermometry. *Agric. Water Mgmt., 95*(10), 1144-1152. https://doi.org/10.1016/j.agwat.2008.04.017

Han, M., Shang, H., DeJonge, K. C., Comas, L. H., & Gleason, S. (2018). Comparison of three crop water stress index models with sap flow measurements in maize. *Agric. Water Mgmt., 203*, 366-375. https://doi.org/10.1016/j.agwat.2018.02.030

Idso, S. B. (1982). Non-water-stressed baselines: A key to measuring and interpreting plant water stress. *Agric. Meteorol., 27*(1-2), 59-70. https://doi.org/10.1016/0002-1571(82)90020-6

Idso, S. B., Jackson, R. D., Pinter, P. J., Reginato, R. J., & Hatfield, J. L. (1981). Normalizing the stress-degree-day parameter for environmental variability. *Agric. Meteorol., 24*, 45-55. https://doi.org/10.1016/0002-1571(81)90032-7

Irmak, S., Haman, D. Z., & Bastug, R. (2000). Determination of crop water stress index for irrigation timing and yield estimation of corn. *Agron. J., 92*(6), 1221-1227. https://doi.org/10.2134/agronj2000.9261221x

Jackson, R. D., William, K. P., & Choudhury, B. J. (1988). A reexamination of the crop water stress index. *Irrig. Sci., 9*, 309-317. https://doi.org/10.1007/BF00296705

Kottek, M., Grieser, J., Beck, C., Rudolf, B., & Rubel, F. (2006). World map of the Köppen-Geiger climate classification updated. *Meteorol. Zeitschrift., 15*(3), 259-263. https://doi.org/10.1127/0941-2948/2006/0130

Lamm, F. R., & Aiken, R. M. (2008). Comparison of temperature-time threshold-and ET-based irrigation scheduling for corn production. ASABE Paper No. 084202. St. Joseph, MI: ASABE.

Ma, X., He, Q., & Zhou, G. (2018). Sequence of changes in maize responding to soil water deficit and related critical thresholds. *Front. Plant Sci., 9*, article 00511. https://doi.org/10.3389/fpls.2018.00511

Nielsen, D. C., & Gardner, B. R. (1987). Scheduling irrigations for corn with the crop water stress index (CWSI). *Appl. Agric. Res., 2*(5), 295-300.

O'Shaughnessy, S. A., & Evett, S. R. (2010). Canopy temperature based system effectively schedules and controls center pivot irrigation of cotton. *Agric. Water Mgmt., 97*(9), 1310-1316. https://doi.org/10.1016/j.agwat.2010.03.012

O'Shaughnessy, S. A., Andrade, M. A., & Evett, S. R. (2017). Using an integrated crop water stress index for irrigation scheduling of two corn hybrids in a semi-arid region. *Irrig. Sci., 35*, 451-467. https://doi.org/10.1007/s00271-017-0552-x

O'Shaughnessy, S. A., Evett, S. R., Colaizzi, P. D., & Howell, T. A. (2012). A crop water stress index and time threshold for automatic irrigation scheduling of grain sorghum. *Agric. Water Mgmt., 107*, 122-132. https://doi.org/10.1016/j.agwat.2012.01.018

Payero, J. O., & Irmak, S. (2006). Variable upper and lower crop water stress index baselines for corn and soybean. *Irrig. Sci., 25*, 21-32. https://doi.org/10.1007/s00271-006-0031-2

Peters, R. T., & Evett, S. R. (2008). Automation of a center pivot using the temperature-time-threshold method of irrigaion scheduling. *J. Irrig. Drain. Eng., 134*(3), 286-291. https://doi.org/10.1061/(ASCE)0733-9437(2008)134:3(286)

R Core Team. (2019). R: A language and environment for statistical computing. Vienna, Austria: R Foundation for Statistical Computing. Retrieved from http://www.R-project.org/

Sabagh, A. E., Barutçular, C., & Islam, M. S. (2017). Relationships between stomatal conductance and yield under deficit irrigation in maize (*Zea mays* L.). *J. Exp. Biol. Agr. Sci., 5*(1), 14-21. https://doi.org/10.18006/2017.5(1).014.021

Shanahan, J. F., & Nielsen, D. C. (1987). Influence of growth retardants (anti-gibberellins) on corn vegetative growth,water use, and grain yield under different levels of water stress. *Agron. J., 79*(1), 103-109. https://doi.org/10.2134/agronj1987.00021962007900010022x

Shokrana, M. S. B., & Ghane, E. (2020). Measurement of soil water characteristic curve using HYPROP2. *MethodsX, 7*(2020), 1-17. https://doi.org/https://doi.org/10.1016/j.mex.2020.100840

Steele, D. D., Stegman, E. C., & Gregor, B. L. (1994). Field comparison of irrigation scheduling method for corn. *Trans. ASAE, 37*(4), 1197-1203.

Taghvaeian, S., Chávez, J. L., & Hansen, N. C. (2012). Infrared thermometry to estimate crop water stress index and water use of irrigated maize in northeastern colorado. *Remote Sens., 4*(11), 3619-3637. https://doi.org/10.3390/rs4113619

Tekelioğlu, B., Büyüktas, D., Bastuğ, R., Karaca, C., Aydinsakir, K., & Dinç, N. (2017). Use of crop water stress index for irrigation scheduling of soybean in mediterranean conditions. *J. Exp. Agric. Intl., 18*(6), 1-8. https://doi.org/10.9734/JEAI/2017/37058

Ünlü, M., Kanber, R., Koç, D. L., Tekin, S., & Kapur, B. (2011). Effects of deficit irrigation on the yield and yield components of drip irrigated cotton in a mediterranean environment. *Agric. Water Mgmt., 98*(4), 597-605. https://doi.org/10.1016/j.agwat.2010.10.020

USDA. (2017). 2017 Census of Agriculture. Washington, DC: USDA-NASS. Retrieved from https://www.nass.usda.gov/Publications/AgCensus/2017/index.php

USDA. (2018). 2018 Irrigation and Water Management Survey. Washington, DC: USDA-NASS. Retrieved from https://www.nass.usda.gov/Surveys/Guide_to_NASS_Surveys/Farm_and_Ranch_Irrigation/

Usman, M., Ahmad, A., Ahmad, S. ,Arshad, M., Khaliq, T., Wajid, A., ..., Hoogenboom, G. (2009). Development and application of crop water stress index for scheduling irrigation in cotton (*Gossypium hirsutum* L.) under semiarid environment. *J Food, Agric. Environ., 7*(3-4), 386-391.

van Genuchten, M. T. (1980). A closed-form equation for predicting the hydraulic conductivity of unsaturated soils. *SSSA J., 44*(5), 892-898. https://doi.org/10.2136/sssaj1980.03615995004400050002x

Wanjura, D. F., & Upchurch, D. R. (1997). Accounting for humidity in canopy-temperature-controlled irrigation scheduling. *Agric. Water Mgmt., 34*(3), 217-231. https://doi.org/10.1016/S0378-3774(97)00024-3

Wanjura, D. F., Upchurch, D. R., & Mahan, J. R. (1992). Automated irrigation based on threshold temperature. *Trans. ASAE, 35*(1), 153-159.

Wanjura, D. F., Upchurch, D. R., & Mahan, J. R. (1995). Control of irrigation scheduling using temperature-time thresholds. *Trans. ASAE, 38*(2), 403-409. https://doi.org/10.13031/2013.16409

Yazar, A., Howell, T. A., Dusek, D. A., & Copeland, K. S. (1999). Evaluation of crop water stress index for LEPA irrigated corn. *Irrig. Sci., 18*, 171-180. https://doi.org/10.1007/s002710050059